

assignment shown based on chemical shifts is reasonable and also agrees with that of Wynberg and co-workers.<sup>27</sup>

**Cyclic Voltammetry.** The electrochemical instrumentation and procedures for resistance compensation were the same as described previously.<sup>43</sup> The digital data acquisition system was used for most of the voltammograms which were to be compared with simulations though some were recorded with a Houston "omnigraphic" X-Y recorder (<0.5 V/s) or Tektronix 5000 storage oscilloscope (>0.5 V/s) followed by digitization of the data. The background-corrected voltammograms were smoothed<sup>44</sup> and compared with the simulations.<sup>21</sup>

A standard three electrode cell was used. Nitrogen, air, or oxygen was admitted through a needle in a septum and expelled through a mineral oil bubbler. The working electrode was a platinum disk sealed in soft glass. It was polished with 5.0 and 0.3 micron alumina on a polishing cloth between voltammograms. The counter electrode was a coiled 1-in. length of platinum wire. The reference electrode was a Corning ceramic junction SCE which was placed in a compartment separated from the test solution by a cracked glass bead. Temperature control was by way of

an external cooling bath, typically dry ice/acetone. The cell was equipped with a small Teflon-coated stirring bar, and the sample was stirred between scans. The special procedures needed to obtain electrochemical data with methylene chloride solvent and with methylene chloride/trifluoroacetic anhydride/trifluoroacetic acid solvent both at room temperature and at -78 °C are fully described elsewhere.<sup>21</sup>

**Acknowledgment.** We thank the Petroleum Research Fund, administered by the American Chemical Society, and the National Science Foundation for partial financial support of this work and the Amoco Oil Company and the Wisconsin Alumni Research Foundation for fellowships to D.L.K. We thank Mark F. Teasley for the CV work on 14 and 15.

**Registry No.** 1, 30541-56-1; 1<sup>+</sup>, 70535-07-8; 2, 35544-39-9; 5 (OMe), 89543-36-2; 5 (Cl), 79732-69-7; 5 (Cl)<sup>+</sup>, 104418-84-0; 5 (O<sub>2</sub>CCF<sub>3</sub>), 104335-93-5; 6 (OMe), 104335-94-6; 7, 77331-40-9; 7<sup>+</sup>, 104418-85-1; 8, 55993-21-0; 9, 100208-23-9; 9<sup>+</sup>, 100296-10-4; 10, 100208-24-0; 10<sup>+</sup>, 100296-11-5; 11, 51689-29-3; 12, 30614-34-7; 13, 88656-03-5; 14, 73321-28-5; 15, 73679-39-7; 16, 7090-88-2; 17, 65498-90-0; 18, 29309-28-2; 19, 20441-18-3; 20, 104335-95-7; 21, 99810-86-3; 22, 104335-96-8.

(43) O'Connell, K. M.; Evans, D. H. *J. Am. Chem. Soc.* **1983**, *105*, 1473.

(44) Fitch, A.; Evans, D. H. *J. Electroanal. Chem.*, in press.

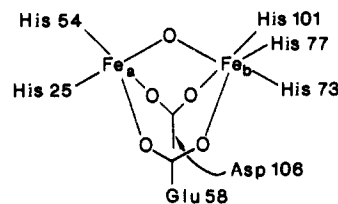
## <sup>1</sup>H NMR Probes of the Binuclear Iron Cluster in Hemerythrin

Michael J. Maroney,<sup>†‡</sup> Donald M. Kurtz, Jr.,\*<sup>†</sup> Judith M. Nocek,<sup>‡</sup> Linda L. Pearce,<sup>‡</sup> and Lawrence Que, Jr.\*<sup>†</sup>

Contribution from the Departments of Chemistry at the University of Minnesota, Minneapolis, Minnesota 55455, and Iowa State University, Ames, Iowa 50010. Received April 14, 1986

**Abstract:** <sup>1</sup>H NMR spectroscopy has been used to probe the various redox states of hemerythrin (Hr) to gain insight into the structural and magnetic changes that may occur in these states. In all, three oxidation states have been studied: deoxy [Fe(II),Fe(II)], semimet [Fe(II),Fe(III)], and met and oxy [Fe(III),Fe(III)]. The solvent-exchangeable imidazole NH protons of histidine ligands to the metal centers can be observed in all these complexes. For the met and oxy forms of the protein, these protons are found near 20 ppm, a shift significantly decreased from that found in mononuclear high-spin ferric imidazole complexes (ca. 100 ppm). This decrease in shift is consistent with the strong antiferromagnetic coupling ( $J = -100 \text{ cm}^{-1}$ ) found for these complexes. For the deoxyHr complexes, the NH shifts range from 40 to 80 ppm, values comparable to those found for mononuclear high-spin ferrous complexes. This result shows the iron centers in the deoxy forms are not strongly coupled. Evans' susceptibility measurements on deoxyHr and deoxyHrX (X = N<sub>3</sub><sup>-</sup>, NCO<sup>-</sup>, F<sup>-</sup>) show the presence of a weak antiferromagnetic interaction ( $J = -15 \text{ cm}^{-1}$ ) in deoxyHr and even weaker interactions in deoxyHrX ( $J = -11, -5, 0 \text{ cm}^{-1}$  for X = F<sup>-</sup>, NCO<sup>-</sup>, N<sub>3</sub><sup>-</sup>, respectively). For the semimetHr complexes, the NH shifts are also indicative of weak coupling. In all complexes except  $\mu$ -SsemimetHr,  $J$  is estimated to be ca.  $-20 \text{ cm}^{-1}$  from the temperature dependences of the shifts of the Fe(III)-coordinated imidazole NH's. The NMR spectra also show that the iron atoms have a trapped valence formulation on the NMR time scale, with the anion coordinated to the ferric center. The small  $J$  values found for the deoxyHr and semimetHr complexes are consistent with the  $J$  values found for synthetic Fe(III)-Fe(III) and Fe(II)-Fe(II) complexes with  $\mu$ -hydroxo-di- $\mu$ -acetato bridging units and suggest that the oxo bridge found in the met and oxy forms of hemerythrin has become protonated upon reduction. The persistence of a bridge between the metal centers in the various states of hemerythrin would facilitate the electron transfer required for reversible oxygenation. The NMR data support the mechanism proposed by Stenkamp et al. (*Proc. Natl. Acad. Sci. U.S.A.* **1985**, *82*, 713-716) for reversible oxygenation wherein the proton on the hydroxo bridge of deoxyHr is transferred to the bound peroxide as deoxyHr is converted to oxyHr. The stability of the semimetHrX complexes suggests that semimetHr superoxide [Fe(II),Fe(III)O<sub>2</sub><sup>-</sup>] is a reasonable transition state in the oxygenation process.

Hemerythrin (Hr), a respiratory protein isolated from a number of marine invertebrates, contains a binuclear non-heme iron oxygen-binding site.<sup>1</sup> The structures of the iron clusters in oxyHr, metHr, and metHrN<sub>3</sub>, where both iron atoms are high-spin ferric centers, have been well-characterized by X-ray crystallographic studies<sup>2-4</sup> and have recently been modelled by synthetic complexes.<sup>5,6</sup> The structure of metHr that emerges from these studies and physical studies of the active site<sup>7-16</sup> (1) has one five-coordinate iron atom (Fe<sub>a</sub>) and one six-coordinate iron atom (Fe<sub>b</sub>). The two



iron atoms are bridged by two carboxylate ligands, one each from glutamate and aspartate residues, and an oxo group. The presence

<sup>†</sup>University of Minnesota.

<sup>‡</sup>Iowa State University.

\*Present address: Department of Chemistry, University of Massachusetts, Amherst, MA 01003.

(1) Klotz, I. M.; Kurtz, D. M., Jr. *Acc. Chem. Res.* **1984**, *17*, 16-22. Sanders-Loehr, J.; Loehr, T. M. *Adv. Inorg. Biochem.* **1979**, *1*, 235-252.

of the oxo group results in a high degree of antiferromagnetic coupling between the ferric centers in oxyHr ( $J = -77 \text{ cm}^{-1}$ ),<sup>13</sup> metHr ( $J = -134 \text{ cm}^{-1}$ ),<sup>13</sup> and metHrX complexes with a variety of small anionic ligands. Five of the remaining six coordination sites are occupied by histidine imidazole groups bound through the nitrogen. The vacant site on Fe<sub>a</sub> in metHr is occupied by peroxide in oxyhemerythrin and by various anions in metHr complexes (e.g., N<sub>3</sub><sup>-</sup> in metHrN<sub>3</sub>). A binuclear site with several spectroscopic features in common with metHr has been characterized in *E. coli* ribonucleotide reductase B2 subunits,<sup>17,18</sup> and similar sites may also exist in other proteins such as methane monooxygenase,<sup>19</sup> uteroferrin,<sup>20</sup> and beef spleen purple acid phosphatase.<sup>20</sup>

The structures of the deoxy<sup>4,21-23</sup> and semimet<sup>16,24,25</sup> forms of hemerythrin are less well-characterized, and detailed structural information is a recent development. The EPR spectra of semimetHr complexes clearly show that antiferromagnetic coupling of the iron sites persists, although the extent of coupling in the semimet site is not apparent from the EPR data.<sup>25</sup> MCD studies have demonstrated that the binuclear iron cluster in deoxyHr has a diamagnetic ground state and thus remains antiferromagnetically coupled ( $J = -13 \pm 5 \text{ cm}^{-1}$ ).<sup>22</sup> The coupling constant obtained ( $J = -13 \pm 5 \text{ cm}^{-1}$ ) is deemed too large to result solely from carboxylate bridges and requires the retention of the exogenous bridge.<sup>22</sup> The apparent absence of an oxo bridge as demonstrated by EXAFS<sup>21</sup> together with the MCD data suggests that the exogenous bridge is modified in deoxyHr.

We have briefly reported the presence of paramagnetically shifted ligand proton resonances in the <sup>1</sup>H NMR spectra of hemerythrin containing binuclear Fe clusters in all three known oxidation states.<sup>16,23</sup> We report here the use of <sup>1</sup>H NMR spec-

troscopy to probe the magnetic properties of the binuclear Fe sites in several semimetHr complexes and in deoxyHr and deoxyHrX complexes. The magnetic information obtained, coupled with the assignment of ligand proton resonances, is then analyzed in terms of the structure of the binuclear iron sites of semimet and deoxy forms of hemerythrin and provides insight into the mechanism for reversible dioxygen binding by hemerythrin.

## Experimental Section

**A. Sample Preparation.** Oxyhemerythrin was isolated in crystalline form from the marine worms *Phascolopsis gouldii* and *Themiste zostericola* by using literature procedures.<sup>26</sup> Concentrations of Hr are expressed in terms of binuclear iron sites. These were determined at 355 nm for metHr and 500 nm for oxyHr.<sup>11</sup> <sup>1</sup>H NMR spectra were obtained on 4 mM solutions of oxyHr in 50 mM phosphate buffer (pH 7.5). Solutions of metHr were prepared by dialyzing ca. 5 mL of solutions of oxyHr (~2 mM) against 1 L of a 1 mM solution of K<sub>3</sub>Fe(CN)<sub>6</sub> in 50 mM phosphate buffer to which NaClO<sub>4</sub> (50 mM) had been added to eliminate the high pH form of metHr and to enhance the stability of the protein solution.<sup>27</sup> After the oxidation was complete, the excess K<sub>3</sub>Fe(CN)<sub>6</sub> was removed by dialysis with a minimum of two 1-L changes of buffer. Stock solutions of ~2 mM metHr in this buffer were stable at 4 °C for several weeks. MetHrX complexes were prepared by adding an excess of anion, as the sodium or potassium salt, directly to stock solutions of metHr. Typical anion concentrations were 0.1 M for NaN<sub>3</sub> and 1 M for all other anions employed. Samples of μ-SmetHr were prepared by oxidizing 1–2 mL samples of 2 mM μ-SsemimetHr (vide infra) by dialysis against 1 L of 1 mM K<sub>3</sub>Fe(CN)<sub>6</sub> in the buffer described above under anaerobic conditions.<sup>28</sup> The samples employed in NMR experiments were subsequently concentrated by using a Minicon concentrator (Amicon) to yield 0.3–0.5 mL of ca. 4 mM solutions of metHr complexes. Resonances assigned to exchangeable protons (histidine imidazole NH protons) were identified by examining the spectra of oxyHr, metHr, μ-SmetHr, and metHrN<sub>3</sub> in H<sub>2</sub>O and then by diluting these samples with 5 mL of the same buffer prepared by using D<sub>2</sub>O and re-concentrating twice. The resonances corresponding to histidine imidazole NH protons in other metHrX complexes were assigned by analogy to these spectra.

Samples of deoxyHr were prepared by two methods. The first consisted of anaerobic dialysis of 1–3 mL of 2–4 mM oxyHr or metHr solutions against 1 L of 5–10 mM solutions of dithionite in 50 mM phosphate buffer (pH 7.5), followed by the removal of excess dithionite from the sample by dialysis against the buffer (2 × 1 L). The second method involved the addition of ca. 3 reducing equiv of a dithionite buffer solution to anaerobic 3 mM solutions of oxyHr or metHr. Addition of Na<sub>2</sub>SO<sub>4</sub> to the buffer was frequently employed to increase the solubility of deoxyHr. In the presence of 0.2 M Na<sub>2</sub>SO<sub>4</sub>, a 3 mM solution of deoxyHr could be prepared and maintained over the course of an NMR experiment. The <sup>1</sup>H NMR spectra obtained for deoxyHr were not sensitive to the presence or absence of NaClO<sub>4</sub>, Na<sub>2</sub>SO<sub>4</sub>, or unreacted dithionite. DeoxyHrX complexes were prepared from the deoxyHr samples by syringe addition of small aliquots of concentrated, anaerobic solutions of anions as sodium or potassium salts. Final anion concentrations from 0.1–1 M were employed to prepare NMR samples of deoxyHr complexes. The resonances assigned to the exchangeable histidine imidazole NH protons in deoxyHr and deoxyHrN<sub>3</sub> were identified as described above; the corresponding resonances in other deoxyHr complexes were assigned by analogy.

The samples of deoxyHr and deoxyHrX complexes used for Evans susceptibility measurements were prepared by the anaerobic dialysis method in D<sub>2</sub>O containing 3 mM DSS. The final concentration of the deoxyHr in the sample was determined to be 3.16 mM by converting a small portion of the sample to oxyHr and measuring the absorbance at 500 nm.<sup>11</sup> The deoxyHr sample was then divided among five NMR tubes (0.4 mL each), each with an insert containing a sample of the D<sub>2</sub>O buffer following dialysis. To four of these tubes, 10 μL of buffer saturated with KF, KOCN, KCl, or NaN<sub>3</sub> was added slowly via syringe. The final concentrations of anions in each sample were the following: F<sup>-</sup>, 0.4 M; OCN<sup>-</sup>, 0.2 M; Cl<sup>-</sup>, 0.1 M; and N<sub>3</sub><sup>-</sup>, 0.2 M. The formation of the complexes was monitored by using the upfield shifted nonexchangeable proton resonances, which indicated that complex formation was complete in each case.

(26) Klotz, I. M.; Klotz, T. A.; Fiess, H. A. *Arch. Biochem. Biophys.* **1957**, *68*, 284–299.

(27) Garbett, K.; Darnall, D. W.; Klotz, I. M. *Arch. Biochem. Biophys.* **1971**, *142*, 455–470.

(28) Lukat, G. S.; Kurtz, D. M., Jr.; Shiemke, A. K.; Loehr, T. M.; Sanders-Loehr, J. *Biochemistry* **1984**, *23*, 6416–6422.

(2) Stenkamp, R. E.; Sieker, L. C.; Jensen, L. H. *J. Am. Chem. Soc.* **1984**, *106*, 618–622.

(3) Hendrickson, W. A. In *Invertebrate Oxygen-Binding Proteins: Structure, Active Site, and Function*; Lamy, J., Lamy, J., Eds.; Marcel-Dekker: New York, 1981; pp 503–515.

(4) Stenkamp, R. E.; Sieker, L. C.; Jensen, L. H.; McCallum, J. D.; Sanders-Loehr, J. *Proc. Natl. Acad. Sci. U.S.A.* **1985**, *82*, 713–716.

(5) Armstrong, W. H.; Spool, A.; Papefthymiou, G. C.; Frankel, R. B.; Lippard, S. J. *J. Am. Chem. Soc.* **1984**, *106*, 3653–3667.

(6) Wieghardt, K.; Pohl, K.; Gebert, W. *Angew. Chem., Int. Ed. Engl.* **1983**, *22*, 727–728. Toftlund, H.; Murray, K. S.; Zwack, P. R.; Taylor, L. F.; Anderson, O. P. *J. Chem. Soc., Chem. Commun.* **1986**, 191–193.

(7) Freier, S. M.; Duff, L. L.; VanDuynne, R. P.; Klotz, I. M. *Biochemistry* **1979**, *18*, 5372–5377. Freier, S. M.; Duff, L. L.; Shriver, D. F.; Klotz, I. M. *Arch. Biochem. Biophys.* **1980**, *205*, 449–463.

(8) Shjemke, A. K.; Loehr, T. M.; Sanders-Loehr, J. *J. Am. Chem. Soc.* **1984**, *106*, 4951–4956.

(9) Sanders-Loehr, J.; Loehr, T. M.; Mauk, A. G.; Gray, H. B. *J. Am. Chem. Soc.* **1980**, *102*, 6992–6996.

(10) Okamura, M. Y.; Klotz, I. M.; Johnson, C. E.; Winter, M. R. C.; Williams, R. J. P. *Biochemistry* **1969**, *8*, 1951–1958.

(11) Garbett, K.; Darnall, D. W.; Klotz, I. M.; Williams, R. J. P. *Arch. Biochem. Biophys.* **1969**, *103*, 419–434.

(12) Gay, R. R.; Solomon, E. I. *J. Am. Chem. Soc.* **1978**, *100*, 8323–8325.

(13) Dawson, J. W.; Gray, H. B.; Hoenig, H. E.; Rossman, G. R.; Schredder, J. M.; Wang, R. H. *Biochemistry* **1972**, *11*, 461–465.

(14) Elam, W. T.; Stern, E. A.; McCallum, J. D.; Sanders-Loehr, J. *J. Am. Chem. Soc.* **1982**, *104*, 6369–6373.

(15) Hendrickson, W. A.; Co, M. S.; Smith, J. L.; Hodgson, K. O.; Klippenstein, G. L. *Proc. Natl. Acad. Sci. U.S.A.* **1982**, *79*, 6255–6259.

(16) Maroney, M. J.; Lauffer, R. B.; Que, L., Jr.; Kurtz, D. M., Jr. *J. Am. Chem. Soc.* **1984**, *106*, 6445–6446.

(17) Lammers, M.; Follman, H. *Struct. Bonding (Berlin)* **1983**, *54*, 27–91.

(18) Sjöberg, B. M.; Graslund, A. *Adv. Inorg. Biochem.* **1983**, *5*, 87–110.

(19) Woodland, M. P.; Dalton, H. *J. Biol. Chem.* **1984**, *259*, 53–59. Woodland, M. P.; Cammack, R. In *Microbial Gas Metabolism: Mechanistic, Metabolic, and Biotechnological Aspects*; Poole, R. K., Dow, C. S., Eds.; Academic Press: New York, 1985; pp 209–213.

(20) Antanaitis, B. C.; Aisen, P. *Adv. Inorg. Biochem.* **1983**, *5*, 111–136.

(21) Elam, W. T.; Stern, E. A.; McCallum, J. D.; Sanders-Loehr, J. *J. Am. Chem. Soc.* **1983**, *105*, 1919–1923.

(22) Reem, R. C.; Solomon, E. I. *J. Am. Chem. Soc.* **1984**, *106*, 8323–8325.

(23) Nocek, J. M.; Kurtz, D. M., Jr.; Sage, J. T.; Debrunner, P. G.; Maroney, M. J.; Que, L., Jr. *J. Am. Chem. Soc.* **1985**, *107*, 3382–3384.

(24) Wilkins, R. G.; Harrington, P. C. *Adv. Inorg. Biochem.* **1983**, *5*, 51–85.

(25) Muhoberac, B. B.; Wharton, D. C.; Babcock, L. M.; Harrington, P. C.; Wilkins, R. G. *Biochim. Biophys. Acta* **1980**, *626*, 337–345.

Samples of semimetHr were prepared by first concentrating an aliquot of stock metHr solution to 4–5 mM, degassing, and adding 1 equiv of dithionite in a buffer solution to the anaerobic protein sample. Solutions of dithionite (ca. 0.03 equiv/L) were prepared and subsequently titrated anaerobically against lumiflavin acetate by monitoring the 444-nm absorption ( $\epsilon$  11 800 cm<sup>-1</sup> M<sup>-1</sup>) of the flavin.<sup>29a</sup> After addition of 1 equiv of dithionite to the metHr samples, the solutions stood at room temperature for 5–10 min to allow complete formation of semimetHr to occur prior to the addition of a small volume of a concentrated, anaerobic solution of a sodium or potassium salt of the desired anion. The final concentrations of semimetHrX were in the 3–4 mM range, with [X] = 0.1 M (X = N<sub>3</sub><sup>-</sup>, CN<sup>-</sup>, and OCN<sup>-</sup>) and [X] = 1 M (X = Cl<sup>-</sup>, F<sup>-</sup>, and OCN<sup>-</sup>).  $\mu$ -SsemimetHr was prepared by the addition of a fourfold excess of NaHS as an anaerobic buffer solution to a 3–4 mM solution of metHr.<sup>29b</sup> X-band EPR spectra (Bruker ER220D spectrometer) obtained at 4 K for semimetHrN<sub>3</sub> and  $\mu$ -SsemimetHr prepared by the methods described were identical with the spectra obtained for samples prepared under more dilute conditions. Double integration of the EPR spectra with copper sulfate as the standard<sup>29c</sup> gave concentrations of semimetHr species that were in good agreement with those obtained by calculations based on the initial concentration of metHr obtained from spectrophotometric measurements.<sup>11</sup>

**B. NMR Measurements.** <sup>1</sup>H NMR spectra were obtained on a Nicolet NT-300 FT NMR spectrometer operating in the quadrature mode (<sup>1</sup>H frequency, 300 MHz). Spectra were collected by using a one pulse sequence with a 90° pulse of 8  $\mu$ s. Spectra obtained on aqueous samples employed a 30-ms presaturation pulse (30–50 dB) from the decoupler to saturate the water and diamagnetic proton resonances. Between 30 000 and 60 000 transients were accumulated over a 30-kHz bandwidth for oxyHr, metHr, and metHrX and over a 50-kHz bandwidth for deoxyHr, deoxyHrX, and semimetHrX samples. The spectra contained 8k data points, and the signal-to-noise ratio was improved by apodization of the free induction decay, which introduced a negligible 10-Hz line broadening. External DSS was used as a shift reference except where otherwise noted.

Areas and line widths of peaks corresponding to histidine imidazole NH protons were determined by using the NTCCAP routine of the Nicolet software to fit the observed peaks to Lorentzian lines. This program was also used to determine chemical shifts for exchangeable protons, particularly in temperature dependence studies and in cases of overlapping peaks. The estimated error in the chemical shift of a peak is in part due to the broadness of the resonance. For metHr complexes with very broad resonances in a region requiring rather severe base line correction, the error is estimated to be ca.  $\pm$ 0.5 ppm. The chemical shifts of exchangeable resonances observed for deoxyHr, deoxyHrX, and semimetHrX are generally reproducible to  $\pm$ 0.2–0.3 ppm, depending on line width. Nonexchangeable resonances with upfield shifts in the deoxyHr, deoxyHrX, and semimetHrX spectra are reproducible to  $\pm$ 0.1 ppm.

Spectra obtained for  $\mu$ -SsemimetHr by using various pulse sequences to null the H<sub>2</sub>O signal gave spectra which were identical with those obtained by using the presaturation technique. This information indicates that the histidine imidazole NH protons are not in rapid exchange with solvent protons on the NMR time scale and that saturation transfer is not occurring to an appreciable extent. This result is not unexpected, since the available crystal structures reveal that the binuclear iron sites are buried in the protein.

The temperature dependence of the <sup>1</sup>H NMR spectra of semimetHrX (X = N<sub>3</sub><sup>-</sup>, F<sup>-</sup>, Cl<sup>-</sup>) and for  $\mu$ -SsemimetHr were measured over the minimum temperature range of 25–55 °C. Usually an extension of one or both of these limits could be made, with the lower limit determined by line broadening and the upper limit by the stability of the protein. In all cases, the temperature of the sample was calibrated by using a method involving the shift difference of the methyl and hydroxyl proton resonances of methanol as a function of temperature.<sup>29b</sup> The error in temperature measurements estimated from the standard deviation of replicate temperature calibrations was determined to be  $\leq$   $\pm$ 0.5 °C over the 0–60 °C range. The *J* value for a particular complex was extracted from the temperature dependence of the isotropic shifts by the method described by Lauffer et al.<sup>30</sup> and by using the magnetic susceptibility equations of Wojciechowski.<sup>31</sup> For mixed-valent complexes, the differing contributions of the two metal oxidation states are taken into account in the

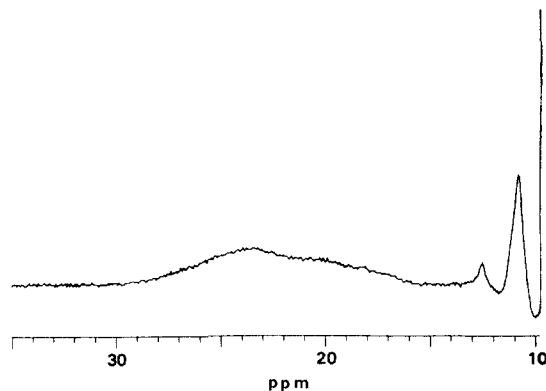


Figure 1. 300-MHz <sup>1</sup>H NMR spectrum of *P. gouldii* oxyhemerythrin at 30 °C.

analysis by using the treatment of Dunham et al.<sup>32</sup> This approach for estimating *J* is best applied to weakly coupled systems, as in the cases of deoxyHr and semimetHrX, where changes in  $\chi$  over a small temperature range are significant. It cannot be reliably applied to oxyHr and metHrX where the coupling is strong, given the available temperature range.

Evans susceptibility measurements on deoxyHr and deoxyHrX samples were carried out in coaxial NMR tubes. The chemical shift difference ( $\Delta\nu$ ) of internal and external DSS at 298 K was measured for samples of deoxyHr and deoxyHrX (X = Cl<sup>-</sup>, F<sup>-</sup>, N<sub>3</sub><sup>-</sup>, OCN<sup>-</sup>) which were obtained from portions of the deoxyHr sample by the addition of a negligible volume of a saturated buffer solution of X. The diamagnetic correction for the protein was obtained by measuring the value of  $\Delta\nu$  for an identical solution of oxyHr obtained from the deoxyHr sample after exposure to air. Values of  $\chi_M$  for deoxyHr and deoxyHrX were then obtained by using eq 1

$$\chi_M = [(3\Delta\nu)/(4\pi\nu_0c)]_{\text{deoxy}} - [(3\Delta\nu)/(4\pi\nu_0c)]_{\text{oxy}} + C \quad (1)$$

where  $\nu_0$  is the spectrometer frequency (300.07 MHz), *c* is the concentration of protein binuclear iron sites, and *C* is the paramagnetic correction for the two antiferromagnetically coupled, high-spin ferric centers in the oxyHr binuclear site ( $3.9 \times 10^{-3}$  cgs/mol at 298 K, assuming a spin only moment with *J* = -77 cm<sup>-1</sup>).<sup>13</sup>

## Results and Discussion

Representative paramagnetic <sup>1</sup>H NMR spectra of various hemerythrin complexes are shown in Figures 1–3. The data from these and other spectra are collected in Table I; only features outside the 0–10 ppm region are tabulated. From the structural information available for hemerythrin, the <sup>1</sup>H NMR spectrum of hemerythrin is expected to contain paramagnetically shifted resonances associated with protons on histidine, aspartate, and glutamate ligands. The resonances associated with the imidazole NH protons of histidine bound to the iron centers are readily assigned by taking advantage of their solvent exchangeability. The assignments of these resonances provide a probe of the magnetic properties and the structure of the binuclear iron cluster in various forms of hemerythrin. (For a discussion of the effects of antiferromagnetic coupling on the <sup>1</sup>H NMR spectra of iron complexes, see ref 33 and the literature cited therein.)

**A. OxyHr and MetHr Complexes.** The <sup>1</sup>H NMR spectra of oxyHr (Figure 1 and Table I) and metHrX (Table I) feature three or four broad, poorly resolved peaks in the 12–25 ppm region associated with solvent-exchangeable protons and a resonance at 11 ppm associated with nonexchangeable protons. The isotropic shifts observed are expected to be predominantly contact in origin because of the <sup>6</sup>A ground electronic state of the high-spin ferric centers.<sup>34</sup> The exchangeable resonances are assigned to the imidazole NH protons of the histidine ligands. (The hydroperoxy proton,<sup>48</sup> if present, would be solvent-exchangeable but is expected

(29) (a) Foust, G. P.; Burleigh, B. D.; Mayhew, S. G.; Williams, C. H.; Massey, V. *Anal. Biochem.* **1969**, *27*, 530–535. (b) Van Geet, A. L. *Anal. Chem.* **1970**, *6*, 679–680. (c) Aasa, R.; Vanngard, T. *J. Magn. Reson.* **1975**, *19*, 308–315.

(30) Lauffer, R. B.; Antanaitis, B. C.; Aisen, P.; Que, L., Jr. *J. Biol. Chem.* **1983**, *258*, 14 212–14 218.

(31) Wojciechowski, W. *Inorg. Chim. Acta* **1967**, *1*, 319–323. Wojciechowski, W. *Inorg. Chim. Acta* **1967**, *1*, 324–328.

(32) Dunham, W. R.; Palmer, G.; Sands, R. H.; Bearden, A. J. *Biochim. Biophys. Acta* **1971**, *253*, 373–384.

(33) Que, L., Jr.; Maroney, M. J. *Metal Ions in Biological Systems*, Vol. 21, in press.

(34) Horrocks, W. D., Jr. In *NMR of Paramagnetic Molecules. Principles and Applications*; LaMar, G. N., Horrocks, W. D., Jr., Holm, R. H., Eds.; Academic Press: New York, 1973; p 128–177.

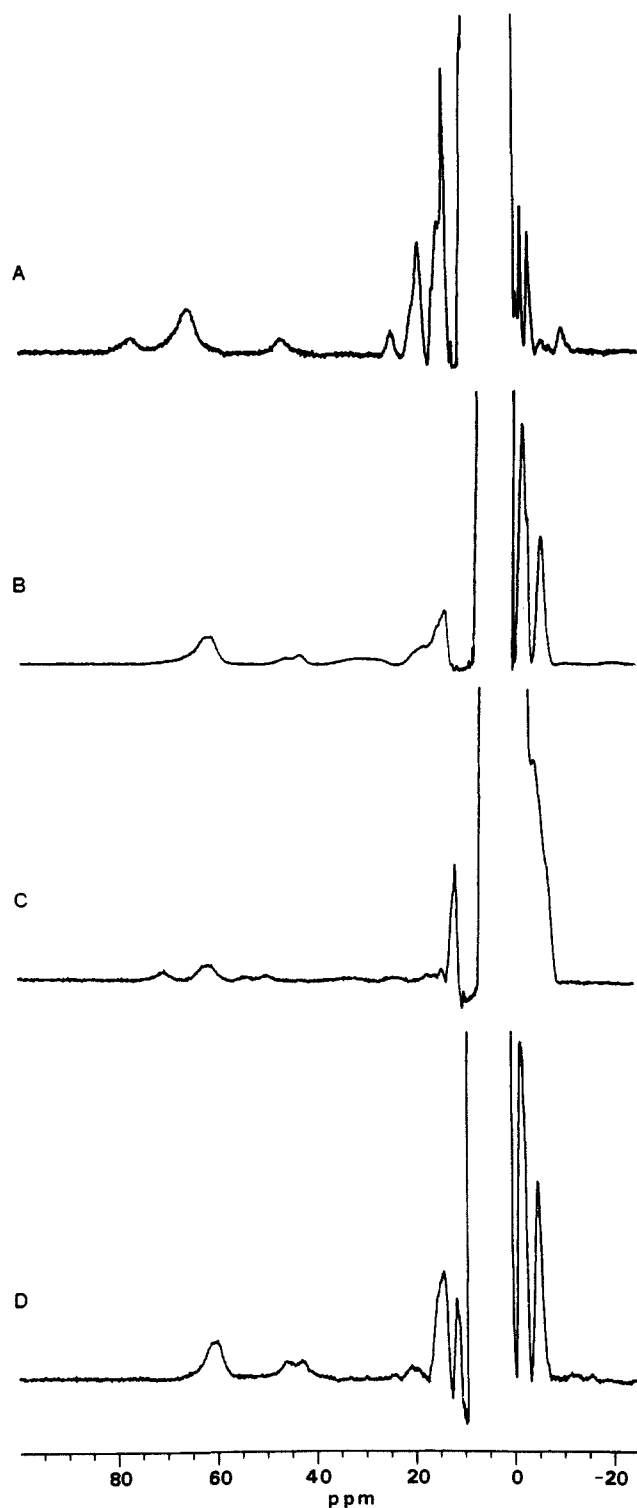


**Figure 2.** 300-MHz  $^1\text{H}$  NMR spectra of *P. gouldii* deoxyhemerythrin and deoxyhemerythrin complexes at 40 °C: A, DeoxyHrN<sub>3</sub>; B, DeoxyHrOCN; C, DeoxyHrF; D, DeoxyHr.

to be too broad to be observed due to its proximity to the binuclear cluster.) The nonexchangeable resonance is assigned to the methylene protons of the carboxylate bridges. This assignment is supported by the spectrum of [(HBpz<sub>3</sub>Fe)<sub>2</sub>O(OAc)<sub>2</sub>],<sup>35</sup> a metHr model compound featuring bridging acetate ligands, which contains a resonance at 10.5 ppm that is unambiguously assigned to the acetate methyl protons.<sup>5</sup> The isotropic shifts of all the observed

(35) Abbreviations used: HBpz<sub>3</sub>, hydrotris(pyrazolyl)borate; OAc, acetate; S<sub>2</sub>-o-xylol, o-xylene- $\alpha,\alpha'$ -dithiolate; salen, *N,N'*-ethylenebis(salicylideneamine); Me<sub>3</sub>tacn, 1,4,7-trimethyl-1,4,7-triazacyclononane; L-Bzim, 2,6-bis[bis(2-benzimidazolylmethyl)aminomethyl]-4-methylphenol.

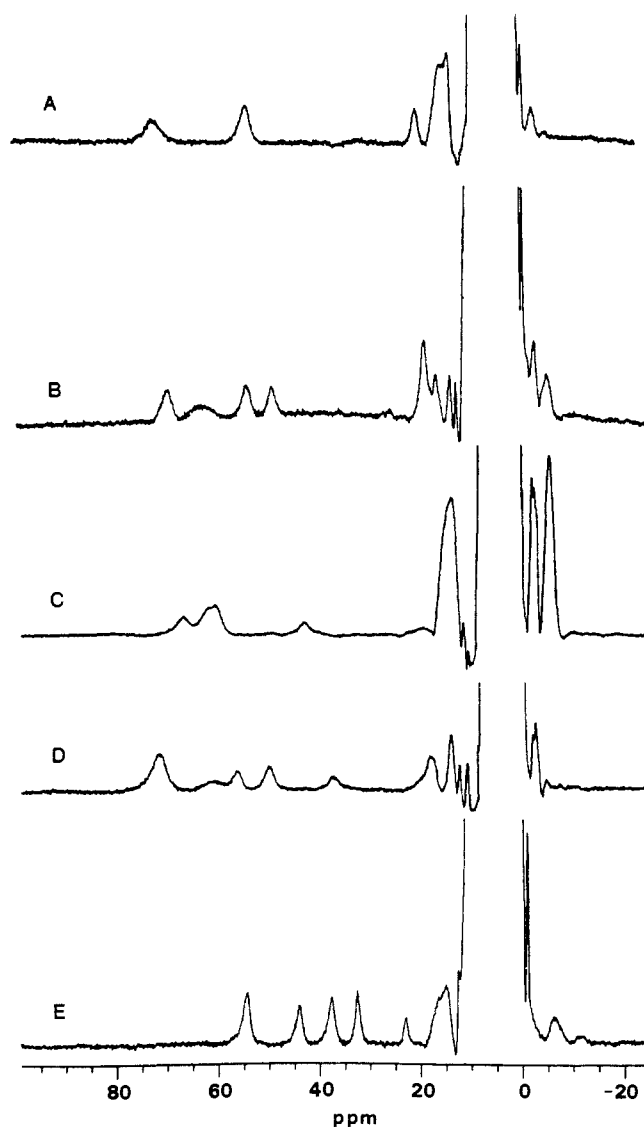


**Figure 3.** 300-MHz  $^1\text{H}$  NMR spectra of *P. gouldii* semimethemerythrin complexes at 40 °C: A, SemimetHrN<sub>3</sub>; B, SemimetHrCl; C, SemimetHrCN; D, SemimetHrF; E,  $\mu$ -SsemimetHr.

oxyHr ligand protons are small compared to those observed for magnetically isolated high-spin ferric complexes (89–96 ppm),<sup>30</sup> a reflection of the strong antiferromagnetic coupling of the ferric sites in oxyHr since contact shifts are proportional to  $\chi$ , the magnetic susceptibility of the cluster. Similar shifts are observed for metHr complexes. Solid susceptibility measurements show that oxyHr and metHr differ somewhat in  $J$  (oxyHr,  $-77\text{ cm}^{-1}$ ; metHr,  $-134\text{ cm}^{-1}$ );<sup>13</sup> the NMR data indicates that this difference is less pronounced.

The pattern of shifts observed for histidine imidazole NH protons of oxyHr is similar to those of all the metHrX complexes studied thus far. The range of shifts observed is probably a result of the low symmetry of the oxyHr and metHrX sites which amplify the anisotropic spin distribution due to the strong antiferromagnetic coupling. As in the case of [Fe(salen)]<sub>2</sub>O,<sup>36</sup> the  $J$  of ca.  $-100\text{ cm}^{-1}$  observed for these complexes results in the occupancy of the  $S' = 0, 1,$  and  $2$  states at ambient temperature. The latter two states have anisotropic spin distributions that place most of the unpaired spin density into particular 3d orbitals that may interact preferentially with one (or more) of the ligands.

The spectra obtained for metHr and  $\mu$ -SmetHr are quite similar to, but differ in detail from, those obtained for oxyHr and metHrX. The fact that the exchangeable proton resonances are observed

(36) LaMar, G. N.; Eaton, G. R.; Holm, R. H.; Walker, F. A. *J. Am. Chem. Soc.* 1973, 95, 63–75.

**Table I.** Chemical Shifts of Proton Resonances in Hemerythrin Complexes

hemerythrin	complex	T (°C)	histidine N-H	chemical shifts (ppm)		
				downfield	upfield	
<i>Phascolopsis gouldii</i>	oxy	30	24, 20 (sh), 18 (sh), 13	11		
	met	30	24, 13	11		
	metCl	40	23, 19, 13	11		
	metF	40	23, 19 (sh), 16, 13	11		
	metOCN	40	23, 19, 13	11		
	metN <sub>3</sub>	30	23, 19, 16, 13	11		
	μ-Smet	10-40	25, 23	11		
	deoxy		62.4, 46.3, 43.2	14, 11	-1.9, -2.5, -3.1, -5.8	
	deoxyCl	40	62.2, 46.5, 43.6	14, 11	-1.9, -2.5, -3.0, -5.9	
	deoxyF	40	70.1, 61.4, 53.6, 49.4	32 (br), 17, 16, 14, 11	-2.2, -2.8, -5.0, -7.4	
	deoxyOCN	40	62 (sh), 60.9, 45.9, 43.1	30 (br), 19 (br), 14, 11	-2.4, -3.3, -6.0	
	deoxyN <sub>3</sub>	40	78.3, 66.8, 47.3	34 (br), 25, 20 (sh), 19 16, 15 (sh), 14	-1.9, -3.3, -10	
	semimetCl	40	70.0, 63 (br), 54.0, 48.8	18, 16, 13, 12	-2.1, -2.8, -5.7	
	semimetF	40	72.1, 60.9, 56.6, 50.2, 37.2	18, 14	-2.9	
	semimetOCN	40	72.0, 68.5, 53.0, 50.5	19, 14	-1.0, -1.7, -3.1	
	semimetN <sub>3</sub>	40	72.2, 53.6	20, 15, 13	-1.1	
	semimetCN	40	67.1, 62 (sh), 60.8, 43.1	13	-2.3, -5.8	
	μ-Ssemimet	40	54.0, 43.6, 37.2, 32.1, 22.5	16, 15, 12	-1.2, -6.1	
	<i>Themiste zostericola</i>	met	40	24, 12	11	
		deoxy	40	66 (sh), 63.1, 60.1, 45.9, 42.8	30 (br), 14, 11	-1.3, -2.7, -3.5, -5, -7
deoxyN <sub>3</sub>		40	79 (br), 67 (br), 46 (br)	25, 19, 16 (sh), 14	-2.4, -3.4, -6.7	
μ-Ssemimet		40	53.9, 43.6, 38.1, 31.9, 22.6	15, 12	-2.9, -3.4, -5.6	

in the same region of the spectrum for μ-SmetHr indicates that the extent of antiferromagnetic coupling is similar to that of other met forms of the protein and that substitution of the μ-oxo group by a μ-sulfido group<sup>28</sup> does not drastically affect the magnetic properties of the cluster. These conclusions are in agreement with expectations based on a comparison of the magnetic properties of the model compounds [Fe(salen)]<sub>2</sub>O ( $J = -95 \text{ cm}^{-1}$ )<sup>37</sup> and [Fe(salen)]<sub>2</sub>S ( $J = -88 \text{ cm}^{-1}$ ).<sup>38</sup> The spectra of metHr and μ-SmetHr, however, contain fewer distinct peaks associated with exchangeable protons than do the spectra of oxyHr or metHrX.

**B. DeoxyHr and DeoxyHrX.** The <sup>1</sup>H NMR spectrum obtained for deoxyHr (Figure 2D, Table I) contains three solvent-exchangeable peaks in the 40–65 ppm region, assigned to histidine imidazole NH protons coordinated to the binuclear metal site in the protein. These shifts, which are only slightly smaller than those found for mononuclear high spin Fe(II) imidazole complexes (57–79 ppm),<sup>30,39</sup> are indicative of a much smaller antiferromagnetic interaction between the iron atoms in the deoxyHr cluster. The peak observed near 62 ppm is substantially larger than the two peaks and is attributed to three NH protons. The wide range of isotropic shifts observed for these peaks suggests the involvement of a significant dipolar component, which is not unexpected for high-spin ferrous complexes.<sup>34</sup>

The temperature dependences of these resonances are shown in Figure 4. The feature at ca. 62 ppm exhibits a dependence consistent with  $J \sim -10 \text{ cm}^{-1}$ , while the features near 45 ppm show dependences suggestive of  $J \sim -20 \text{ cm}^{-1}$ . The differences in the  $J$  values obtained for these peaks demonstrate the complications that arise from a significant dipolar contribution to the isotropic shift. Contact contributions exhibit a  $T^{-1}$  dependence, whereas dipolar contributions have a  $T^{-2}$  dependence in iron complexes.<sup>40</sup> Nevertheless, both values indicate a substantial weakening of the antiferromagnetic interaction between the iron centers upon conversion of oxyHr to deoxyHr, in agreement with

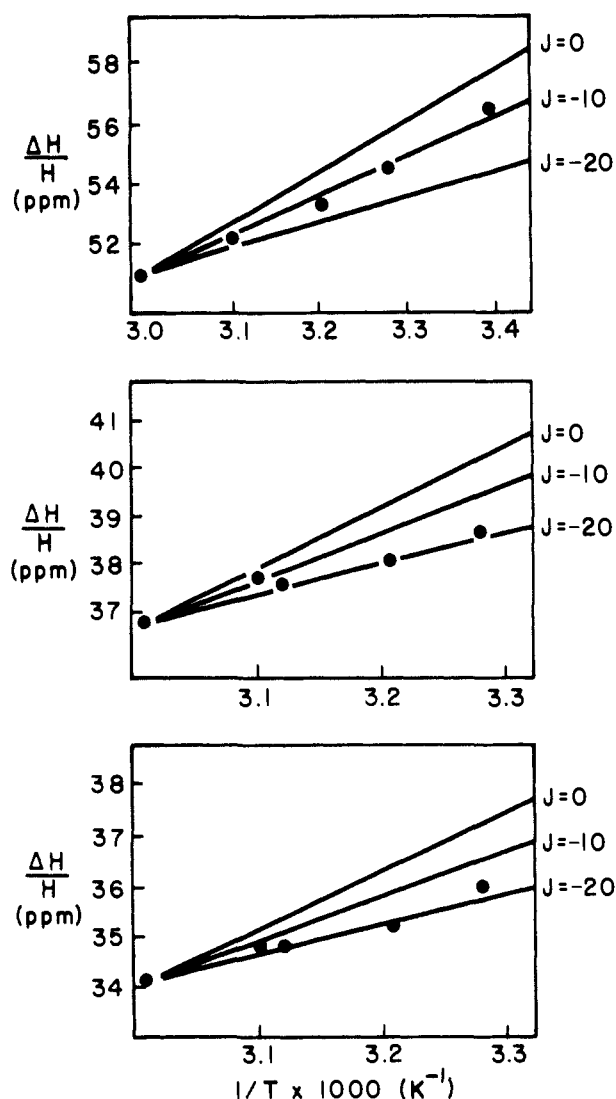


**Figure 4.** The temperature dependence of the isotropic shifts of histidine NH proton resonances in *P. gouldii* deoxyHr.

(37) Wollman, R. G.; Hendrickson, D. N. *Inorg. Chem.* **1977**, *16*, 723–733.

(38) Dorfman, J. R.; Girerd, J. J.; Simhon, E. D.; Stack, T. D. P.; Holm, R. H. *Inorg. Chem.* **1984**, *23*, 4407–4412.

(39) Inubushi, T.; Yonetani, T. *FEBS Lett.* **1983**, *160*, 287–290.

(40) Goff, H. M. In *Iron Porphyrins*; Lever, A. B. P., Gray, H. B., Eds.; Addison-Wesley: Reading, MA, 1983; Part I, 237–281. LaMar, G. N.; Walker, F. A. In *The Porphyrins*; Dolphin, D., Ed.; Academic Press: New York, 1979; Vol. IV, 61–157.

**Table II.** Coupling Constants for Deoxyhemerythrin Complexes from Evans' Susceptibility Difference Measurements

complex	$\Delta\nu_{\text{DDS}}$ (Hz)	$(3\Delta\nu/4\pi)\nu_{\text{oc}}$ ( $10^{-2}$ cgs/ mol/Fe)	$\chi_{\text{m}}$ ( $10^{-2}$ cgs/ mol/Fe)	$J$ ( $\text{cm}^{-1}$ )
deoxyHrN <sub>3</sub>	94 ± 2	2.37 ± 0.03	2.51 ± 0.06	(0) <sup>a</sup>
deoxyHrOCN	84 ± 2	2.11 ± 0.03	2.25 ± 0.06	-5 ± 1
deoxyHrF	73 ± 2	1.84 ± 0.03	1.98 ± 0.05	-11 ± 1
deoxyHrCl	64 ± 2	1.61 ± 0.03	1.75 ± 0.05	-16 ± 2
deoxyHr	66 ± 2	1.66 ± 0.03	1.80 ± 0.05	-15 ± 2
oxyHr	9 ± 2	0.25 ± 0.03	(0.39) <sup>b</sup>	(-77) <sup>b</sup>

<sup>a</sup> Complex has a paramagnetic ground state. <sup>b</sup> Obtained from ref 13.

the isotropic shift observations. These observations are also consistent with MCD results on deoxyHr showing a  $J$  value of  $-13 \pm 5 \text{ cm}^{-1}$ .<sup>22</sup>

The spectrum of deoxyHr also contains several nonexchangeable resonances that experience both upfield and downfield isotropic shifts of much smaller magnitudes. Although these resonances cannot presently be assigned to specific ligand protons, they provide a highly reproducible "fingerprint" that is characteristic of the deoxyHr form present in the sample, particularly the sharp resonances that are shifted upfield ( $-1.0$  to  $-10$  ppm) in the spectra of deoxyHr and deoxyHrX.

The effect of binding anions to the deoxyHr binuclear iron site can be seen by comparing the spectra in Figure 2. Anions that are known to bind to the deoxy site ( $X = \text{N}_3^-$ ,  $\text{OCN}^-$ ,  $\text{F}^-$ )<sup>22,24,41</sup> induce spectral changes, while anions such as  $\text{Cl}^-$  do not affect the <sup>1</sup>H NMR spectrum. The addition of  $\text{N}_3^-$  to deoxyHr gives rise to the largest change in the spectrum. The resonances assigned to histidine imidazole NH protons occur over a wide range from 45 to 80 ppm, and there is an apparent shift of one peak from near 45 ppm in the deoxyHr spectrum to near 80 ppm. Several new nonexchangeable proton resonances are observed in the 14–35 ppm region of the spectrum, where no peaks are observed in the deoxyHr spectrum. In comparison with the deoxyHr spectrum, the number and intensity of peaks in the upfield region of the spectrum of deoxyHrN<sub>3</sub> is greatly reduced. These spectral changes suggest that the coordination of azide, presumably to Fe<sub>a</sub>, significantly alters the geometry about that iron site, thus altering the dipolar effect experienced by the protons near the active site.

The spectra observed for deoxyHrX ( $X = \text{F}^-$ ,  $\text{OCN}^-$ ) display more subtle changes. Both complexes show some resolution of one of the NH resonances occurring in the envelope near 62 ppm in the deoxyHr spectrum, and both display a unique pattern of resonances in the upfield region and several peaks in the 14–35 ppm region of their spectra. The paucity of NMR data on synthetic Fe(II) complexes precludes further interpretation of our results.

Reem and Solomon have concluded from EPR and MCD studies of deoxyHrN<sub>3</sub> that, upon the binding of azide, the two iron centers become six-coordinate and the antiferromagnetic coupling between the ferrous centers becomes small relative to the zero-field splitting of the individual centers.<sup>22</sup> Because of the large magnetic moments of the weakly coupled high-spin ferrous centers present in deoxyHr and deoxyHrX and the low susceptibility of the highly coupled oxyHr binuclear site, we have also probed the magnetic interaction of the iron atoms in deoxyHr and deoxyHrX by using Evans' susceptibility difference measurements. The results of these measurements on 3.16 mM samples of protein are shown in Table II. The conditions for the Evans' experiments allowed us to monitor the upfield regions of the samples studied to ascertain that the complexes were fully formed. Values of  $\Delta\nu$  of 60–90 Hz were observed for the reduced proteins, compared with a value of 9 Hz for oxyHr. The value of  $\chi_{\text{M}}$  calculated for deoxyHrN<sub>3</sub> ( $2.51 \times 10^{-2}$  cgs/mol) falls in the range expected for magnetically isolated, high-spin Fe(II) complexes ( $2.19$ – $2.54 \times 10^{-2}$  cgs/mol), in agreement with the MCD results.<sup>22</sup> Values of

$J$  were estimated for deoxyHr and deoxyHrX by assuming that  $J = 0 \text{ cm}^{-1}$  for the deoxyHrN<sub>3</sub> iron cluster and that the spin-orbit contribution to the susceptibility is a constant for the reduced clusters. The value of  $J$  calculated for deoxyHr by using this approach ( $J = -15 \pm 2 \text{ cm}^{-1}$ ) is in excellent agreement with the value obtained from the temperature dependence of the MCD spectrum of the protein. The addition of  $\text{Cl}^-$  to deoxyHr does not affect the coupling of the iron centers, in agreement with expectations based on the <sup>1</sup>H NMR spectrum of deoxyHr in the presence of  $\text{Cl}^-$  (vide supra) and the MCD studies.<sup>22</sup> The addition of anions known to form complexes with the deoxyHr iron cluster reduces the antiferromagnetic interaction by varying amounts ( $J = -11 \pm 1 \text{ cm}^{-1}$ ,  $X = \text{F}^-$ ;  $J = -5 \pm 1 \text{ cm}^{-1}$ ,  $X = \text{OCN}^-$ ), indicating that the antiferromagnetic interaction of the iron centers is quite sensitive to the nature of the anion present. These results suggest the persistence of a bridging group in the deoxyHrX complexes that is capable of mediating the antiferromagnetic interaction of the iron atoms. Since the acid forms of these anions have been shown to be the reactive species in the formation of deoxyHrX,<sup>41b</sup> perhaps the variable extent of coupling observed reflects the partial protonation of the hydroxo bridge upon binding HX.

The X-ray crystallographic information available for the deoxyHr active site indicates that few structural differences exist between oxyHr and deoxyHr.<sup>4</sup> Analysis of the EXAFS spectrum of deoxyHr indicates that an oxo bridge is not present.<sup>21</sup> It is likely that this bridge has become protonated in deoxyHr, as suggested by the significantly smaller antiferromagnetically coupling. Further support for this can be found in the synthesis of a model for deoxyHr, a binuclear Fe(II) complex bridged by hydroxide and two carboxylates, which exhibits a  $J$  of  $-13 \text{ cm}^{-1}$ .<sup>42</sup>

**C. SemimetHrX.** Reduction of metHr or oxidation of deoxyHr by one electron gives rise to the mixed valent [Fe(III),Fe(II)] clusters found in semimetHr complexes.<sup>25,43,44</sup> EPR spectra obtained at low temperature ( $<30 \text{ K}$ ) are characteristic of an antiferromagnetically coupled binuclear iron cluster with an  $S = 1/2$  ground state.<sup>25</sup> Under certain conditions, the semimet species generated by reduction and by oxidation can be distinguished by their characteristic EPR spectra.<sup>25,44</sup> The addition of a ligand to either semimet form produces a single species—semimetHrX.<sup>45,46</sup> These complexes give rise to large chemical shifts for the histidine NH protons (75–35 ppm) in the <sup>1</sup>H NMR spectra of the proteins, as shown for semimetHrX ( $X = \text{N}_3^-$ ,  $\text{OCN}^-$ ,  $\text{F}^-$ ,  $\text{Cl}^-$ ,  $\text{CN}^-$ ) in Figure 3 and Table I. Several nonexchangeable proton resonances shifted either upfield or downfield by small amounts are also observed in these spectra.

We have previously reported on two distinct types of spectra observed for semimetHr complexes, those of semimetHrN<sub>3</sub> and  $\mu$ -SsemimetHr.<sup>16</sup> The spectrum obtained for semimetHrN<sub>3</sub> features two groups of resonances near 72 and 54 ppm at 40 °C assigned to histidine imidazole NH protons. Comparisons of these shifts with those expected for the NH protons of the imidazole ligands in magnetically isolated high-spin ferric and ferrous complexes (100 and 65 ppm, respectively) indicate that the histidine ligands bound to the ferric and ferrous iron centers are easily distinguished, giving rise to the peaks at 72 and 54 ppm, respectively. This assignment is consistent with the line widths observed for the two peaks, which should reflect the spin state of the iron center involved.<sup>47</sup> The difference in line width expected is small compared to the uncertainty of measuring broad lines (600–1000 Hz), making quantitative measurements difficult.

(42) Chaudhuri, P.; Wiegardt, K.; Nuber, B.; Weiss, J. *Angew. Chem., Intl. Ed. Engl.* **1985**, *24*, 778–779.

(43) Harrington, P. C.; DeWaal, D. J. A.; Wilkins, R. G. *Arch. Biochem. Biophys.* **1978**, *191*, 444–451.

(44) Bradić, Z.; Harrington, P. C.; Wilkins, R. G. *Biochemistry* **1980**, *19*, 4149–4155. Babcock, L. M.; Bradić, Z.; Harrington, P. C.; Wilkins, R. G.; Yoneda, G. S. *J. Am. Chem. Soc.* **1980**, *102*, 2849–2850.

(45) Harrington, P. C.; Wilkins, R. G.; Muhoberac, B. B.; Wharton, D. C. In *The Biological Chemistry of Iron*; Dunford, H. B., et al., Eds.; De Reidel: Dordrecht, Holland, 1982; pp 145–160.

(46) Harrington, P. C.; Wilkins, R. G. *J. Am. Chem. Soc.* **1981**, *103*, 1550–1556.

(47) Swift, T. J. in ref 34, p 53–83.

(41) (a) Bradić, Z.; Conrad, R.; Wilkins, R. G. *J. Biol. Chem.* **1977**, *252*, 6069–6075. (b) Bradić, Z.; Tsukahara, K.; Wilkins, P. C.; Wilkins, R. In *Frontiers in Bioinorganic Chemistry*; Xavier, A. V., Ed.; VCH: Weinheim, FRG, 1986; pp 336–344.

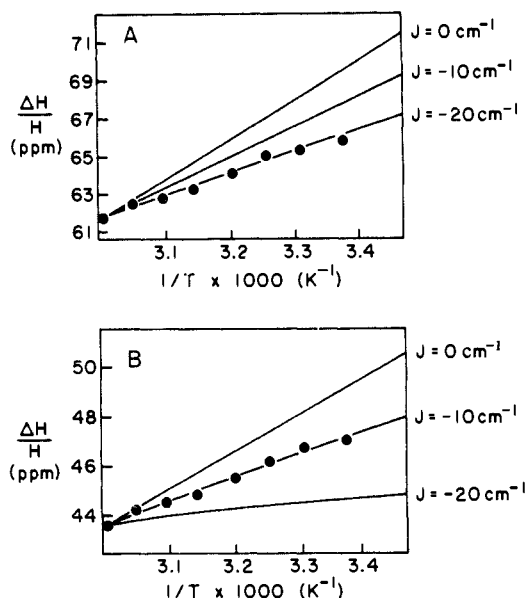


**Figure 5.** The temperature dependence of the isotropic shifts of histidine NH proton resonances in *P. gouldii* semimetHrN<sub>3</sub>: A, ferric histidine ligands; B, ferrous histidine ligands.

However, the peak at 72 ppm is broader than the peak at 54 ppm at all temperatures (10–55 °C), as expected for a proton associated with the more paramagnetic metal center. The peaks are relatively sharp at higher temperatures and become very broad at temperatures less than 20 °C. This trend is a general feature of semimetHr and deoxyHr spectra and suggests that the rotational correlation time of the octameric protein (MW = 108 000) is a factor in determining the observed line widths via the Curie mechanism.<sup>48</sup> In general, the line widths of the resonances observed for exchangeable protons in semimetHrX are narrower than those of the correspondings metHr or deoxyHr complexes. The line widths are decreased because the antiferromagnetically coupled cluster adopts a  $T_{1c}$  that is equal to or less than that of the shorter  $T_{1c}$  of the isolated metal centers.<sup>49</sup> Given that the  $T_{1c}$  of magnetically dilute ferrous complexes are ca.  $10^{-12}$  s and those for ferric complexes fall in the  $10^{-9}$ – $10^{-11}$  s range, the predicted trends in line widths (metHr > deoxyHr ≥ semimetHr) agree well with those observed in the spectra of the proteins.

The observation of separate histidine imidazole NH resonances for the iron centers in semimetHrN<sub>3</sub> indicates a trapped mixed-valent complex exists in the protein. Temperature dependence studies show no indication of a dynamic process. Given the assignments discussed above and the known structure of metHr, it is possible to distinguish between Fe<sub>a</sub> and Fe<sub>b</sub> in semimetHrN<sub>3</sub>. The ratio of the area under the peak at 72 ppm to the area of the 54 ppm peak is 2:3. Thus, Fe<sub>a</sub> is the ferric center and Fe<sub>b</sub> is the ferrous center. This assignment is consistent with the persistence of the  $\text{N}_3^- \rightarrow \text{Fe}^{3+}$  charge-transfer transition in the electronic absorption spectrum of semimetHrN<sub>3</sub>.<sup>50</sup>

The observation of the ferric (and ferrous) histidine NH resonances at lower chemical shifts than in magnetically isolated complexes is consistent with the presence of antiferromagnetic coupling of the iron centers in the mixed-valent clusters. Estimates of the magnitude of the coupling constant may be obtained from comparison of the expected shifts for histidine ligands in mononuclear iron complexes and those observed in semimetHrN<sub>3</sub> or from the observed temperature dependence of isotropic shifts of the histidine ligand resonances. In either case, the ferric peak provides the more reliable measure of the coupling. For the

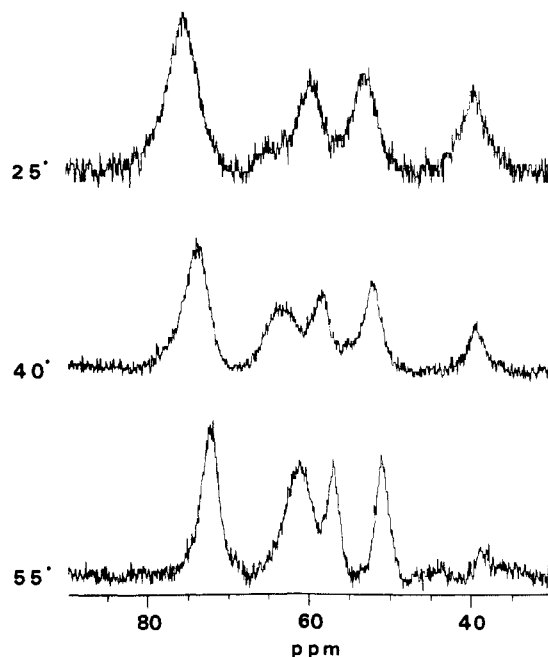


**Figure 6.** The temperature dependence of the  $^1\text{H}$  NMR spectrum of histidine NH resonances in the *P. gouldii* semimetHrF binuclear iron sites.

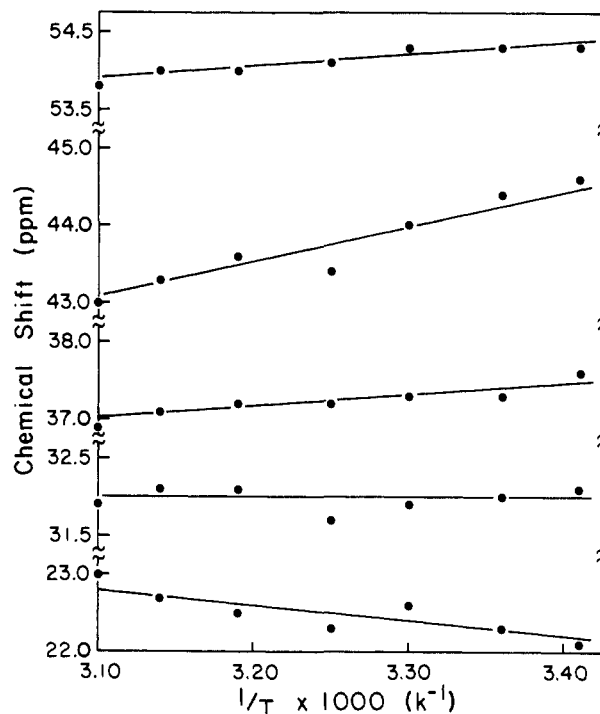


**Figure 7.** The temperature dependence of the isotropic shift of histidine NH proton resonances in *P. gouldii*  $\mu$ -SsemimetHr.

isotropic shift comparisons, the range of imidazole NH shifts found for magnetically isolated ferric complexes is much narrower than for ferrous complexes<sup>30</sup> and provides a more accurate measure of the decrease in the shift (decrease in  $\chi_M$ ) in the coupled cluster. Furthermore, the temperature dependence of the ferric peak is expected to be less complicated by dipolar contributions than that of the ferrous site.<sup>33</sup>

The decrease in the contact shift experienced by the ferric ligand protons in the semimetHrN<sub>3</sub> site indicates a reduction in the susceptibility of the ferric center of 32%.<sup>51</sup> This corresponds to

(51) The number was obtained by comparing the imidazole N–H isotropic shift in semimetHrN<sub>3</sub> with that for a mononuclear ferric complex assuming 8 ppm as the diamagnetic position for a coordinated imidazole NH. Thus  $1 - [(72 - 8)/(102 - 8)] = 0.32$ .

(48) Gueron, M. J. *J. Magn. Reson.* **1975**, *19*, 58–66.

(49) Benelli, C.; Dei, A.; Gatteschi, D. *Inorg. Chem.* **1982**, *21*, 1284–1286. Dei, A.; Gatteschi, D.; Piergentili, E. *Inorg. Chem.* **1979**, *18*, 89–93. Bertini, I.; Lanini, G.; Luchinat, C.; Mancini, M.; Spina, G. *J. Magn. Reson.* **1985**, *65*, 56–63.

(50) Irwin, M. J.; Duff, L. L.; Shriver, D. F.; Klotz, I. M. *Arch. Biochem. Biophys.* **1983**, *224*, 473–478.

the reduction in susceptibility expected for the ferric component of a mixed-valent cluster with a  $J$  of ca.  $-18 \text{ cm}^{-1}$ .<sup>52</sup> A similar result, independent of model compound data, can be obtained from an analysis of the temperature dependence of the ferric peak. The peak displays a Curie temperature dependence that can be fit with a curve corresponding to  $J = -20 \pm 3 \text{ cm}^{-1}$  (Figure 5). A similar analysis of the temperature dependence of the ferrous peak is consistent with a  $J = -10 \pm 2 \text{ cm}^{-1}$  (Figure 7). The lower absolute value of  $J$  obtained from the temperature dependence of the ferrous peak is consistent with the presence of a small downfield dipolar contribution to the isotropic shift experienced by the ferrous histidine imidazole NH resonances.

The spectra obtained for other semimetHrX ( $X = \text{F}^-, \text{Cl}^-, \text{CN}^-, \text{OCN}^-$ ) (Figure 3, Table I) are not as simple as that observed for semimetHrN<sub>3</sub>. All of the semimetHrX complexes except  $X = \text{N}_3^-$  exhibit 4–5 exchangeable resonances in the 35–75 ppm region of the spectrum. Within the framework of the model where isotropic shifts of protons on histidine ligands of a ferric center result solely from a contact mechanism while those on a ferrous center may include contributions from dipolar components, a single semimet site could give rise to four histidine imidazole NH resonances if the Fe center with the exogenous ligand, Fe<sub>a</sub>, is the ferric center (2 his, unresolved) and Fe<sub>b</sub> is the ferrous center (3 his, possibly resolved by differing dipolar components arising from different geometrical factors), as found in semimetHrN<sub>3</sub>. The similarity of the isotropic shifts observed to those of semimetHrN<sub>3</sub> indicates that the antiferromagnetic coupling between the two metal centers is not dramatically altered when N<sub>3</sub><sup>-</sup> is replaced with other anions. Measurements on the semimetHrX complexes ( $X = \text{Cl}^-, \text{F}^-$ ) reveal that all the NH peaks exhibit Curie temperature dependence, by analogy with those of semimetHrN<sub>3</sub>; analysis of data shows  $J$  values of  $-16 \pm 3$  and  $-23 \pm 3 \text{ cm}^{-1}$  for semimetHrCl and semimetHrF, respectively.

The values of  $J$  determined for semimetHr complexes resemble those found for synthetic diiron complexes bridged by hydroxide and two carboxylates, e.g., [(HBpz<sub>3</sub>Fe)<sub>2</sub>OH(OAc)<sub>2</sub>]<sup>+</sup> ( $J = -17 \text{ cm}^{-1}$ )<sup>53</sup> and [(Me<sub>3</sub>tacnFe)<sub>2</sub>OH(OAc)<sub>2</sub>]<sup>+</sup> ( $J = -13 \text{ cm}^{-1}$ ),<sup>42</sup> regardless of the iron oxidation states. Recently a mixed-valent complex with iron centers presumably bridged by phenolate and two benzoates, [Fe<sub>2</sub>(L-Bzim)(O<sub>2</sub>CPh)<sub>2</sub>](BF<sub>4</sub>)<sub>2</sub>, has been characterized with a  $J$  value of  $-5 \text{ cm}^{-1}$ .<sup>54</sup> The model compound data indicate that the nature of the bridging groups plays a more important role than the formal oxidation states of the iron centers in determining the degree of antiferromagnetic coupling in the binuclear iron sites. Because of the similarity of the  $J$  values, it would appear that the iron sites in semimetHr complexes are also bridged by hydroxide and two carboxylates. The absence of an oxo bridge is also suggested by the disappearance of the Fe–O–Fe stretch in the resonance Raman spectrum of semimetHrN<sub>3</sub>.<sup>50</sup> Thus the conversion of metHr to semimetHr would simply require a one-electron reduction and the protonation of the oxo bridge.

The spectra obtained for semimetHrF and  $\mu$ -SsemimetHr each contain five exchangeable proton resonances and cannot be interpreted as arising from a single semimet site by using the model described above. The temperature dependence of the semimetHrF spectrum (Figure 6) exhibits clear evidence for the involvement of two semimet forms in equilibrium with each other. At 40 °C, the spectrum contains histidine imidazole NH resonances at 72, 61, 57, 50, and 37 ppm. At 25 °C, the peak at 61 ppm is almost absent, its presence suggested only by a small shoulder on the peak near 57 ppm. The ratio of the areas of the four peaks at 25 °C is close to 2:1:1:1, consistent with a single semimetHr site. The line widths observed for the peaks (1150, 800, 850, and 850 Hz, respectively) are consistent with the assignment of the peak at 72 ppm to ferric histidine ligands and the other peaks to ferrous histidine ligands. As the temperature is raised, the peak at 61

ppm grows in, and the peak at 37 ppm decreases in size. Cooling the sample reverses the process, demonstrating an equilibrium that can be perturbed by changes in temperature near room temperature. The nature of the two species is at present unclear and under further investigation. Possibilities being considered include an equilibrium between Fe<sub>a</sub><sup>III</sup>Fe<sub>b</sub><sup>II</sup> and Fe<sub>a</sub><sup>II</sup>Fe<sub>b</sub><sup>III</sup> forms and an interchange between the terminal fluoride and the bridging hydroxide. We note also that two forms of metHrF have been distinguished with CD experiments.<sup>11</sup> If the two forms of semimetHrF and metHrF are derived from similar chemistry, the former possibility would be considered unlikely.

The spectrum of  $\mu$ -SsemimetHr (Figure 3E), where the native oxygen bridging group has been replaced by a sulfur bridging group,<sup>28</sup> also features five exchangeable proton resonances near 54, 44, 38, 32, and 23 ppm at 40 °C. The isotropic shifts exhibited by these proton resonances are not as great as those in semimetHrF and other semimetHrX complexes, indicating that  $-J$  for the sulfur-bridged species is larger than for the hydroxo-bridged semimet forms. The isotropic shifts of the histidine protons in the 0–60 °C temperature range exhibit little temperature dependence (Figure 7), indicating that the coupling between the metal centers is of such a magnitude that the Néel point of the susceptibility curve is near ambient temperature. For an Fe(III)–Fe(II) complex, this would correspond to a  $J$  of ca.  $-30 \text{ cm}^{-1}$ . Within the errors associated with these measurements, it is possible to identify peaks exhibiting both Curie (54, 44, 38 ppm) and anti-Curie temperature dependences (23 ppm) in the spectrum—a feature reminiscent of reduced 2Fe ferredoxins.<sup>32,55</sup> The larger coupling observed for  $\mu$ -SsemimetHr relative to the semimetHrX complexes probably arises from the persistence of the sulfido bridge. Resonance Raman spectra of  $\mu$ -SsemimetHr show no shift in the symmetric Fe–S–Fe stretch in D<sub>2</sub>O,<sup>28,56</sup> indicating that the bridging sulfide is not protonated. The two- to threefold decrease in the extent of antiferromagnetic coupling upon reduction of  $\mu$ -SmetHr to  $\mu$ -SsemimetHr must be due predominantly to formal reduction of one of the two iron atoms of  $\mu$ -SmetHr, in analogy to similar changes in  $J$  for the oxidized and reduced forms of the two-iron ferredoxins.<sup>57</sup>

The temperature dependence of the  $\mu$ -SsemimetHr spectrum does not reveal an obvious equilibrium like that exhibited by semimetHrF. The ratio of the areas of the five peaks in the spectrum at 40 °C is ca. 3:2:2:2:1 and is temperature independent. The line widths observed for the NH peaks at 40 °C are 400, 375, 375, 250, and 250 Hz, respectively, much narrower than other semimetHrX complexes. Although we are unable to demonstrate the presence of an equilibrium between more than one  $\mu$ -SsemimetHr form, the observation of five histidine imidazole NH resonances in the spectrum with the associated intensities suggests the presence of more than one species (vide supra). The areas of the peaks suggest the presence of a 50/50 mixture of the two semimet forms. This result is in contrast to the Mossbauer spectrum of this complex at liquid helium temperatures, which shows the presence of only one species.<sup>58</sup>

We are currently investigating the NMR spectra of (semimet)<sub>R</sub>Hr and (semimet)<sub>O</sub>Hr to gain insight into the differences between these complexes, but we are as yet unable to interpret our results. Our efforts are continuing.

**D. *Themiste zostericola* Hemerythrin.** We have begun to explore the variations in the structure of the binuclear iron complex that may occur in proteins from different sources. The <sup>1</sup>H NMR

(52) This was computed by using the equations of Wojciechowski<sup>31</sup> and the treatment of Dunham et al. on mixed-valent Fe(III)–Fe(II) clusters.<sup>32</sup>

(53) Armstrong, W. H.; Lippard, S. J. *J. Am. Chem. Soc.* **1984**, *106*, 4632–4633.

(54) Suzuki, M.; Uehara, A.; Endo, K. *Inorg. Chim. Acta* **1986**, *123*, L9–L10.

(55) (a) Bertini, I.; Lanini, G.; Luchinat, C. *Inorg. Chem.* **1984**, *23*, 2729–2732. (b) Nagayama, K.; Ozaki, Y.; Kyogoku, Y.; Hase, T.; Matsubara, H. *J. Biochem. (Tokyo)* **1983**, *94*, 893–902. (c) Chan, T.-M.; Markley, J. L. *Biochemistry* **1983**, *22*, 6008–6010. (d) Salmeen, I. T.; Palmer, G. *Arch. Biochem. Biophys.* **1972**, *150*, 767–773. (e) Poe, M.; Phillips, W. D.; Glickson, J. D.; McDonald, C. C.; San Pietro, A. *Proc. Natl. Acad. Sci. U.S.A.* **1971**, *68*, 68–71.

(56) Freier, S. M.; Duff, L. L.; Van Duyne, R. P.; Klotz, I. M. *Biochemistry* **1979**, *18*, 5372–5377.

(57) Palmer, G. In *Iron-Sulfur Proteins*; Lovenberg, W., Ed.; Academic Press: New York, 1973; Vol. II, pp 285–325.

(58) Kurtz, D. M., Jr.; Sage, J. T.; Hendrich, M.; Debrunner, P.; Lutak, G. S. *J. Biol. Chem.* **1983**, *258*, 2115–2118.



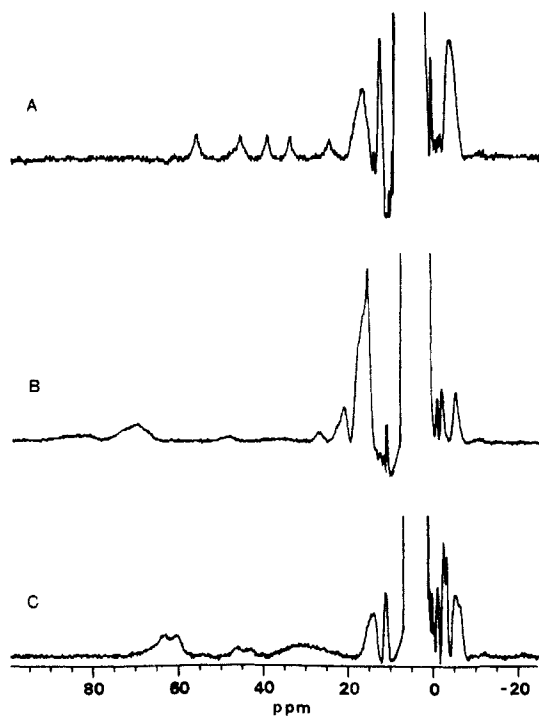


Figure 8. 300-MHz <sup>1</sup>H NMR spectra of *Themiste zostericola* heme-rythrins at 40 °C: A,  $\mu$ -SsemimetHr; B, DeoxyHrN<sub>3</sub>; C, DeoxyHr.

spectra of T.z.  $\mu$ -SsemimetHr, deoxyHrN<sub>3</sub>, and deoxyHr (Figure 8) can be compared with those of corresponding complexes of hemerythrin from *Phascolopsis gouldii* (Figures 2 and 3 and Table I). In general, the spectra are quite similar, the biggest difference being the larger line widths observed for the *Themiste* protein (e.g., T.z.  $\mu$ -SsemimetHr at 40 °C, the five NH resonances have line widths of 375, 475, 450, 375, and 275 Hz). Small differences do exist, such as in the T.z.  $\mu$ -SsemimetHr spectrum where four of the five histidine imidazole NH resonances occur at identical positions as in the P.g. protein at 40 °C, but the middle peak is shifted 1 ppm further downfield in the T.z. spectrum. These results indicate that the binuclear sites in the two proteins are quite similar and that only subtle structural differences exist.

### Conclusions

The mechanism employed by hemerythrin to bind oxygen involves the oxidation of two ferrous iron centers to ferric centers in concert with the two-electron reduction of molecular oxygen to peroxide. The structure of oxyHr,<sup>4,8,12</sup> which features peroxide bound only to Fe<sub>a</sub>, suggests that the electron transfer occurs in two one-electron steps. The possible role of a semimetHr superoxide complex in the oxygen-binding reaction is suggested by the preparation of several semimetHr complexes<sup>24</sup> and the characterization of the NO adduct of deoxyHr as [Fe(II),Fe(III)NO]<sup>-</sup>.<sup>23</sup> The presence of an exogenous bridging group in the binuclear iron sites in all oxidation states may be a critical structural element to the extent that it provides a pathway for the rapid and reversible transfer of electrons between the iron centers and molecular oxygen.

The results reported herein establish two new facts about semimetHrX complexes: (i) the extent of antiferromagnetic exchange coupling in semimetHrX ( $-J \sim 20 \text{ cm}^{-1}$ ) is decreased dramatically compared to that of either metHr ( $134 \text{ cm}^{-1}$ ) or oxyHr ( $77 \text{ cm}^{-1}$ ),<sup>13</sup> (ii) the iron atoms have a trapped valence [Fe(II),Fe(III)] formulation on the NMR time scale ( $\sim 10^{-4}$  s in the case of X = N<sub>3</sub><sup>-</sup>). The trapped valences have been demonstrated previously on the Mossbauer time scale ( $10^{-7}$  s) for  $\mu$ -SsemimetHr.<sup>58</sup>

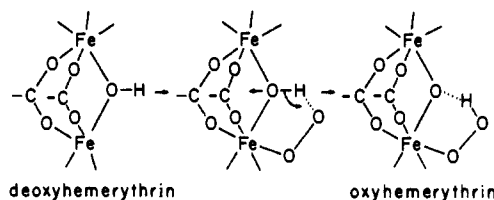


Figure 9. Proposed mechanism of reversible oxygenation of hemerythrin.

In a similar fashion, the antiferromagnetic coupling between the iron atoms in deoxyHr ( $-J = 15 \pm 2 \text{ cm}^{-1}$ ) is dramatically decreased compared to metHr or oxyHr and is essentially non-existent in deoxyHrN<sub>3</sub>. Our results on deoxyHrX complexes confirm and extend those of previous workers.<sup>10,22</sup>

Comparisons with synthetic complexes strongly suggest that these decreases in antiferromagnetic coupling in the semimetHr and deoxy complexes reflect protonation of the oxo group that bridges the iron atoms at the met oxidation level. Otherwise, no major structural changes are observed among the three oxidation levels. This structural constancy would promote reversible dioxygen binding and support the mechanism first proposed by Stenkamp et al.<sup>4</sup> and shown in Figure 9. In this mechanism, the proton associated with the hydroxo bridge in deoxyHr is transferred to dioxygen as it gets reduced; the hydroxo bridge thus becomes an oxo bridge and the dioxygen is transformed into a coordinated hydroperoxide. The hydrogen bonding to the oxo group shown in Figure 9 is apparently not sufficient to affect the extent of antiferromagnetic coupling. Though the solid susceptibility measurements indicate a substantial difference in the coupling in metHr and oxyHr, the NMR spectra of these complexes would suggest that this difference is less dramatic.

The possibility of a semimetHr superoxide species participating in the mechanism for reversible oxygen binding is raised by the relative stability of the semimetHrX complexes. Although there is no evidence for such a species, one could formulate such a complex as [Fe(II),Fe(III)O<sub>2</sub><sup>-</sup>]. Such a complex would differ from the other semimetHrX<sub>2</sub><sup>-</sup> complexes in that the superoxide is capable of accepting another electron to yield oxyHr. Transfer of the proton from the  $\mu$ -hydroxo group to the superoxide might facilitate this latter process. Thus, semimetHr superoxide would at best be a rather fleeting species.

One further implication of our results concerns the kinetics of reduction of Hr from the met to the deoxy oxidation level. Several studies have shown that reduction of met to semimet is almost invariably much faster than reduction of semimet to deoxy.<sup>24,59,60</sup> If the met to semimet reduction is accompanied by protonation of the  $\mu$ -oxo bridge, then no net change in charge on the center need occur. In contrast, further reduction to deoxy without an additional protonation would alter the charge on the cluster and require adjustments by the surrounding protein. The need for such adjustment (i.e., conformational changes) could explain both the slower rate and the zero-order dependence on concentration of reducing agent for the semimet to deoxy step.

**Acknowledgment.** This work has been supported by the National Science Foundation (DMB-8314935, L.Q.) and the National Institutes of Health (GM-33157, D.M.K.). L.Q. is an Alfred P. Sloan Research Fellow and the recipient of an NIH Research Career Development Award. We thank Dr. Gudrun S. Lukat for experimental assistance and helpful discussions.

Registry No. O<sub>2</sub>, 7782-44-7.

(59) Armstrong, G. D.; Ramasami, T.; Sykes, A. G. *Inorg. Chem.* **1985**, *24*, 3230-3234.

(60) Utecht, R. E.; Kurtz, D. M., Jr. *Inorg. Chem.* **1985**, *24*, 4458-4459.